Radiative Capture Cross Sections for Fast Neutrons*

B. C. DIVEN, J. TERRELL, AND A. HEMMENDINGER
Los Alamos Scientific Laboratory, University of California, Los Alamos, New Mexico
(Received June 6, 1960)

Neutron capture cross sections have been measured for 28 elements in the neutron energy range 175 to 1000 kev. The method used was detection of capture gamma radiation in a one-meter-diameter liquid scintillator, the capture samples being placed at the center for irradiation by a pulsed neutron beam. Absolute cross sections have been determined by comparison with the known capture-plus-fission cross section of U^{235}; both capture and fission events are detected with nearly 100% efficiency in this arrangement. Corrections have been made for loss of capture-gamma-ray energy, by means of pulse height analyses and comparison between one-meter and 48-cm scintillator results; corrections have also been made for change in path length due to scattering. The results obtained appear to agree reasonably well with the predictions of resonance theory, with level densities given by the Fermi gas model together with the effective ground state of Hurwitz and Bethe. The low capture cross sections of magic-number target nuclides appear well correlated with the magic-number effects on the mass.

I. INTRODUCTION

CAPTURE cross sections for fast neutrons are of major significance to cosmology[1] and nuclear reaction theory[2] as well as to reactor design. Notwithstanding the unusual interest in these cross sections, it is only within the past few years that effective methods have been developed for making such measurements with meaningful precision and over a wide range of energies and elements.

There are three effects associated with radiative capture which provide means for detecting it. These are as follows:

(1) A neutron is lost. (2) A different nucleus is formed. This nucleus may be either stable or radioactive. (3) Prompt gamma radiation is produced, the total energy release being equal to the binding energy of the neutron in the residual nucleus plus its kinetic energy.

The first effect, neutron loss, has been used in the danger-coefficient and pile-oscillator methods[3–6] to provide a large amount of data on absorption cross sections for thermal neutrons. These measurements depend upon the change in reactivity or local flux produced by the change in position of a substance which captures neutrons. The first effect has also served as the basis of a method, originated at Los Alamos by Hanson, which utilizes the transmission of neutrons from an isotropic source by a thick spherical shell.[6–8] A neutron detector insensitive to energy, such as a long counter, is used to determine the attenuation by the shell. The technique is similar to the shell method of measuring inelastic scattering cross sections.[9,10]

Two types of experiments are based on the second effect, using the detection of the residual nuclei formed in the capture process. In one, a mass spectrometer is used to detect the residual nuclei.[11–15] In order to produce a sufficiently large number of nuclei to be detected, a long irradiation in a high flux is required. The method is useful only with reactor spectra and has not been used to determine cross sections for monoenergetic neutrons. The second method involves detection of the radioactive end product. This procedure allows one to measure activation cross sections, which are often the same as the absorption cross sections. This method can be used with monoenergetic sources of a wide range of energies and can be far more sensitive than any other method of detecting capture. Most capture cross sections have been measured by this

* Work done under the auspices of the U. S. Atomic Energy Commission. Several preliminary reports of this work have been given (references 36–39).

[1] E. M. Burbidge, G. R. Burbidge, W. A. Fowler, and F. Hoyle, Revs. Modern Phys. **29**, 547 (1957).

[2] H. Feshbach, C. E. Porter, and V. F. Weisskopf, Phys. Rev. **96**, 448 (1954).

[3] D. J. Hughes, *Pile Neutron Research* (Addison-Wesley Publishing Company, Inc., Reading, Massachusetts, 1953), pp. 196–206.

[4] J. E. R. Holmes, D. D. McVicar, H. Rose, R. D. Smith, and L. R. Shepherd, *Proceedings of the International Conference on the Peaceful Uses of Atomic Energy, Geneva, 1955* (United Nations, New York, 1956), Vol. 5, p. 331.

[5] H. Rose, J. Nuclear Energy **5**, 4 (1957).

[6] A. I. Leipunsky, O. D. Kazachkovsky, G. Y. Artyukhov, A. I. Baryshnikov, T. S. Belanova, V. N. Galkov, Y. Y. Stavissky, E. A. Stumbur, and L. E. Sherman, *Proceedings of the Second United Nations International Conference on the Peaceful Uses of Atomic Energy, Geneva, 1958* (United Nations, Geneva, 1958), Vol. 15, p. 50.

[7] T. S. Belanova, J. Exptl. Theoret. Phys. (U.S.S.R.) **34**, 574 (1958) [translation: Soviet Phys. JETP **7**, 397 (1958)].

[8] H. W. Schmitt, C. W. Cook, and J. H. Gibbons, Bull. Am. Phys. Soc. **4**, 474 (1959); H. W. Schmitt and C. W. Cook, Nuclear Phys. (to be published).

[9] J. R. Beyster, R. L. Henkel, R. A. Nobles, and J. M. Kister, Phys. Rev. **98**, 1216 (1955).

[10] H. A. Bethe, J. R. Beyster, and R. E. Carter, J. Nuclear Energy **3**, 207, 273 (1956); **4**, 3, 147 (1957).

[11] M. G. Inghram, R. J. Hayden, and D. C. Hess, Phys. Rev. **71**, 643 (1947).

[12] R. E. Lapp, J. R. VanHorn, and A. J. Dempster, Phys. Rev. **71**, 745 (1947).

[13] M. G. Inghram, R. J. Hayden, and D. C. Hess, Phys. Rev. **79**, 271 (1950).

[14] W. R. Kanne, H. B. Stewart, and F. A. White, *Proceedings of the International Conference on the Peaceful Uses of Atomic Energy, Geneva, 1955* (United Nations, New York, 1956), Vol. 4, p. 315.

[15] A. Kafalas, M. Levenson, and C. M. Stevens, Nuclear Sci. and Eng. **2**, 657 (1957).

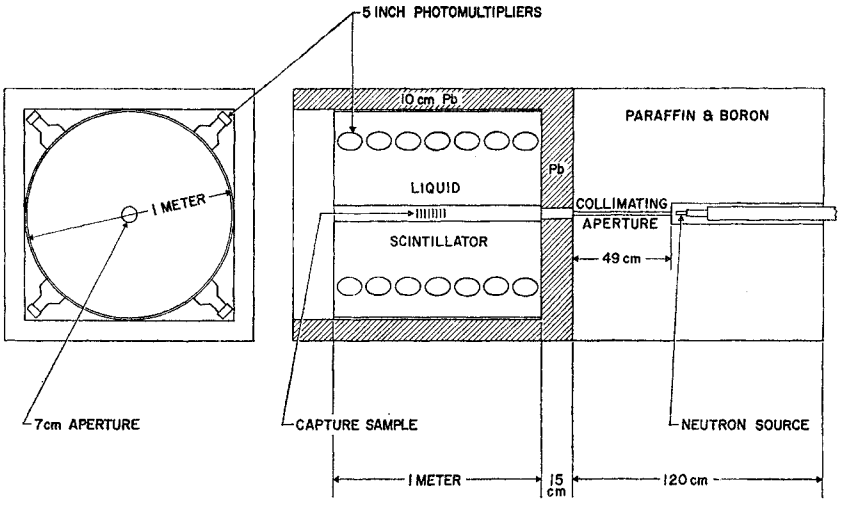

FIG. 1. Experimental arrangement for one-meter-diameter liquid scintillator. Not all of the shielding used is shown.

method.[6,16–31] However, it is applicable only to those nuclides which have a radioactive end product with a suitable half-life.

Two types of observations can be based on the third effect—the prompt capture gamma radiation. One method involves the use of spectrometers[32–34] to study the spectra of gamma radiation. Important information about nuclear energy levels can be obtained, as well as practical information of use in shielding calculations. It is not generally practical to determine capture cross sections by these methods. The other type of observation will be the subject of this paper. It involves absorption of nearly all the gamma radiation regardless of spectrum in a gamma-ray detector so that essentially every capture event may be detected, and the radiative capture cross section thus determined.[35–40]

II. EXPERIMENTAL PROCEDURE

A. General

A method for the measurement of capture cross sections by detection of the capture gamma radiation has been developed at Los Alamos.[35] In these experiments the capture sample is placed at the center of a large liquid scintillator, as in Fig. 1. Ideally, the scintillator should be large enough to absorb all gamma radiation emitted at its center, so that the pulse height would correspond to the sum of the energies of all the gamma rays. This total energy is equal to the binding energy of a neutron in the residual nucleus, plus the kinetic energy of the incident neutron. A collimated beam of neutrons is directed along the axis of the scintillator through a cylindrical channel, passing

[16] H. C. Martin and R. F. Taschek, Phys. Rev. **89**, 1302 (1953).
[17] C. Kimball and B. Hamermesh, Phys. Rev. **89**, 1306 (1953).
[18] D. J. Hughes, R. C. Garth, and J. S. Levin, Phys. Rev. **91**, 1423 (1953).
[19] R. L. Macklin, N. H. Lazar, and W. S. Lyon, Phys. Rev. **107**, 504 (1957); R. L. Macklin, *Proceedings of the Second United Nations International Conference on the Peaceful Uses of Atomic Energy, Geneva, 1958* (United Nations, Geneva, 1958), Vol. 15, p. 68.
[20] R. Booth, W. P. Ball, and M. H. MacGregor, Phys. Rev. **112**, 226 (1958).
[21] J. L. Perkin, L. P. O'Connor, and R. F. Coleman, Proc. Phys. Soc. (London) **A72**, 505 (1958).
[22] V. N. Kononov, Iu. Ia. Stavisskii, and V. A. Tolstikov, Atomnaya Energ. **5**, 564 (1958) [translation: Soviet J. Atomic Energy **5**, 1483 (1959); J. Nuclear Energy **A11**, 46 (1959)].
[23] M. V. Pasechnik, I. F. Barchuk, I. A. Totsky, V. I. Strizhak, A. M. Korolov, Y. V. Hofman, G. N. Lovchikova, E. A. Koltynin, and G. B. Yankov, *Proceedings of the Second United Nations International Conference on the Peaceful Uses of Atomic Energy, Geneva, 1958* (United Nations, Geneva, 1958), Vol. 15, p. 18.
[24] *Neutron Cross Sections*, compiled by D. J. Hughes and R. B. Schwartz, Brookhaven National Laboratory Report BNL-325 (Superintendent of Documents, U. S. Gorernment Printing Office, Washington, D. C., 1958), 2nd ed.
[25] S. J. Bame, Jr., and R. L. Cubitt, Phys. Rev. **113**, 256 (1959).
[26] W. S. Lyon and R. L. Macklin, Phys. Rev. **114**, 1619 (1959).
[27] A. E. Johnsrud, M. G. Silbert, and H. H. Barschall, Phys. Rev. **116**, 927 (1959).
[28] R. C. Hanna and B. Rose, J. Nuclear Energy **8**, 197 (1959).
[29] A. T. G. Ferguson and E. B. Paul, J. Nuclear Energy **A10**, 19 (1959).
[30] J. A. Miskel, K. V. March, M. Lindner, and R. J. Nagle, Bull. Am. Phys. Soc. 4, 475 (1959); University of California Radiation Laboratory Report UCRL-5454, January, 1959 (unpublished).
[31] L. W. Weston, E. G. Bilpuch, K. K. Seth, and H. W. Newson, Bull. Am. Phys. Soc. 4, 475 (1959); Ann. Phys. (to be published).
[32] G. A. Bartholomew and L. A. Higgs, Chalk River Project Report CRGP-784, Ontario, Canada, 1958 (unpublished).
[33] L. V. Groshev, A. M. Demidov, V. N. Lutsenko, and V. I. Pelekhov, *Atlas of γ-Ray Spectra from Radiative Capture of Thermal Neutrons* (Pergamon Press, New York, 1959).
[34] H. T. Motz, R. E. Carter, and P. C. Fisher, Bull. Am. Phys. Soc. 4, 246 (1959); H. T. Motz, R. E. Carter, P. C. Fisher, and W. D. Barfield, Bull. Am. Phys. Soc. 4, 477 (1959); **5**, 246 (1960).
[35] B. C. Diven, J. Terrell, and A. Hemmendinger, Phys. Rev. **109**, 144 (1958).
[36] B. C. Diven, *Proceedings of the Second United Nations International Conference on the Peaceful Uses of Atomic Energy, Geneva, 1958* (United Nations, Geneva, 1958), Vol. 15, p. 60; *Progress in Nuclear Energy*, edited by R. A. Charpie et al. (Pergamon Press, New York, 1959), Ser. I, Vol. 3, p. 125.
[37] B. C. Diven and J. Terrell, Bull. Am. Phys. Soc. 4, 473 (1959).
[38] J. Terrell and B. C. Diven, Bull. Am. Phys. Soc. 4, 475 (1959).
[39] J. Terrell, Argonne National Laboratory Report ANL-6122, 1960 (unpublished), pp. 33-50.
[40] R. L. Macklin, J. H. Neiler, J. H. Gibbons, and P. D. Miller, Bull. Am. Phys. Soc. 4, 43, 385, 414, 474 (1959); Phys. Rev. (to be published).

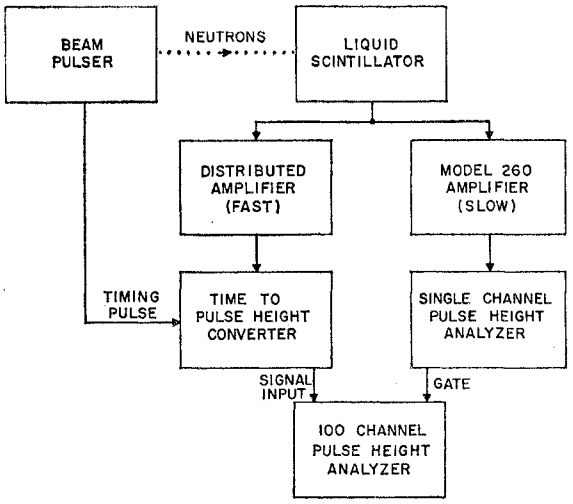

FIG. 2. Schematic arrangement of electronic equipment used in obtaining time distributions of scintillator pulses.

through the sample at the center of the detector. The neutron beam is pulsed so that the neutrons which strike the sample arrive in bursts, the duration of which can be varied between 2 and 10×10^{-8} sec. The time between bursts varies from $\frac{3}{4}$ μsec to 100 μsec.

Pulses in the scintillator which are caused by prompt gamma rays due to capture are essentially coincident with the arrival of the beam pulse at the sample. Other pulses are also produced by scattering, the only interaction other than capture which is produced in most materials by neutrons of energy less than 1 Mev. Although elastic scattering of a neutron by the sample leads to a delayed pulse from neutron capture in the hydrogen of the solution, such scattering provides only a small prompt pulse produced by recoil protons during the slowing down of the neutron in the solution. An inelastic scattering can produce a prompt scintillator pulse due both to gamma radiation and recoil protons, but the sum cannot exceed the neutron energy. If the electronic equipment is required to respond only to prompt pulses which correspond to more than 1 Mev of gamma radiation, all scattering events for 1-Mev neutrons will be ignored, except for random coincidences.

Figure 1 shows the arrangement of neutron source, collimator, scintillator, and some of the shielding. The collimator provides a narrow beam of neutrons which passes through the axial tube of the liquid scintillator. The neutron beam diameter is 1.9 cm at the sample position; the axial opening is 7.0 cm in diameter. The scintillator tank which is shown is a cylinder 1 meter in diameter and 1 meter long, with a white painted interior. The detectors are 28 photomultipliers 5 inches in diameter (DuMont 6364), all mounted on the cylindrical surface of the tank with outputs in parallel. The gains of the photomultiplier tubes are equalized by adjustment of individual voltage dividers. The stabilized high voltage for the tubes is monitored continuously by a differential voltmeter, allowing the voltage to be maintained at 1600 ± 1 volts. The liquid scintillator solution is triethylbenzene and terphenyl, with POPOP as a wavelength shifter. The terphenyl and POPOP constitute 0.3% and 0.01% of the solution by weight. The scintillator tank is shielded by 10 or 15 cm of lead and at least 30 cm of boron-loaded paraffin (not shown) on all sides except the rear.

A capture sample is made in the form of a row of thin disks, 3.8 cm in diameter and spaced at least 3 mm apart for a length of 11 cm in a light aluminum frame. A similar set of polyethylene disks, used to produce scattering only, is mounted in the same way, and a third identical frame, with no sample, is used as a blank. The dimensions and arrangement of the disks are chosen to provide a sample which is as transparent as possible to capture gamma rays and neutrons. The mass of the sample is limited both by the mean free path of primary neutrons and by the need to minimize secondary effects such as the production of capture by scattered neutrons.

A block diagram of the electronic system is shown in Fig. 2. Pulses from the scintillator, amplified by five Hewlett-Packard Model 460 amplifiers, are delivered to a Los Alamos Model 12 time-to-pulse-height converter.[41] A zero of time is established in the converter by a synchronizing pulse from the beam pulser, and the converter then produces an output pulse whose amplitude is proportional to the time interval between the synchronizing pulse and the scintillator pulse. A Los Alamos Model 2A 100-channel pulse-height analyzer then records the time distribution of scintillator pulses.

In order to select the range of scintillator pulse heights which will be acceptable for analysis, a Los Alamos Model 260 amplifier is used to deliver scintillator pulses to a discriminator circuit which selects the desired pulse-height interval. A gating pulse from this circuit is used to gate on the 100-channel pulse-height analyzer, which thus records the time distribution of those scintillator pulses whose heights lie in the selected interval. The purpose of this selection of acceptable pulse heights is to exclude various sorts of background pulses. These include the effects of natural radioactivity, producing a considerable counting rate below about 1 Mev, 2.2-Mev pulses produced by delayed capture of scattered neutrons in the hydrogen of the scintillator solution, and the very large pulses produced by cosmic radiation. In order to exclude these background pulses, and particularly the effects of scattered neutrons, a discriminator interval of 3 to 12 Mev was used for most of the data.

Figure 3 shows a typical set of such data, with the prompt peak due to capture gamma rays from tantalum

[41] W. Weber, C. W. Johnstone, and L. Cranberg, Rev. Sci. Instr. 27, 166 (1956).

superimposed on a background of random pulses in the scintillator. The time interval displayed in the figure is approximately 1 μsec. Also shown is the time distribution of pulses observed with a polyethylene $[(CH_2)_n]$ scatterer in place. In both distributions, and also for the case of no sample, a small peak appears just before "prompt" time. These pulses are ascribed to gamma rays from prompt neutron capture in the collimator near the neutron source, and from proton reactions in or near the Van de Graaff target. There is also a very small peak at prompt time for the blank run, and a somewhat larger peak for polyethylene (not noticeable in Fig. 3), followed by a slightly increased counting rate for a fraction of a microsecond. These effects are believed due to fast capture of scattered neutrons in construction materials of the scintillator tank and in the solution.

The number of prompt counts for any sample which are due to random coincidence may be determined by extrapolating the constant background rate before prompt time into the prompt peak region. The remaining counts are not accidental, but are associated with the beam pulse. The amount of polyethylene is adjusted for each capture sample so as to simulate the scattering effect of the sample, which can readily be determined by the increase in random background when the (nonradioactive) sample is introduced. Thus the polyethylene data should give the number of prompt pulses, after random background subtraction, which are not due to capture in the sample. Prompt capture in the polyethylene itself should be completely negligible.

B. Capture-Pulse-Height Data

Determination of the total number of captures which occurred in the run requires knowledge of the detector efficiency. This is nearly 100% when extrapolated to zero bias. If the capture gamma radiation is emitted in several quanta, some of the energy is virtually certain to be absorbed in the scintillator, although it is also almost certain that some of the radiation will escape. The pulse-height distribution is therefore a continuous one, varying from zero energy to a maximum given by the binding energy of the neutron plus its kinetic energy. An extrapolation must be made in order to account for the small fraction of pulses which lie below the lowest permissible bias setting. For each element and one energy (400 kev) a set of runs was made in which the distribution of pulse heights produced by capture gamma radiation was determined.

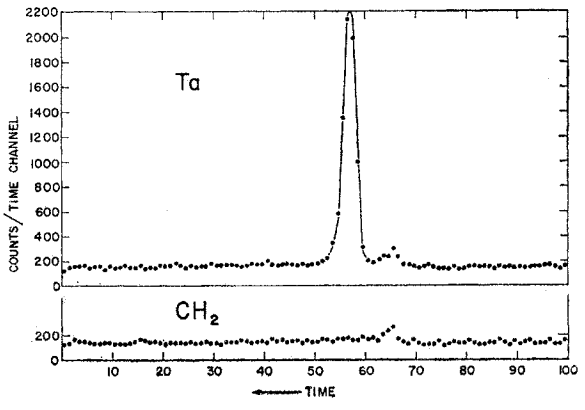

FIG. 3. Typical pulse-time distributions obtained for Ta capture sample and polyethylene scatterer. The time range is about 1 μsec.

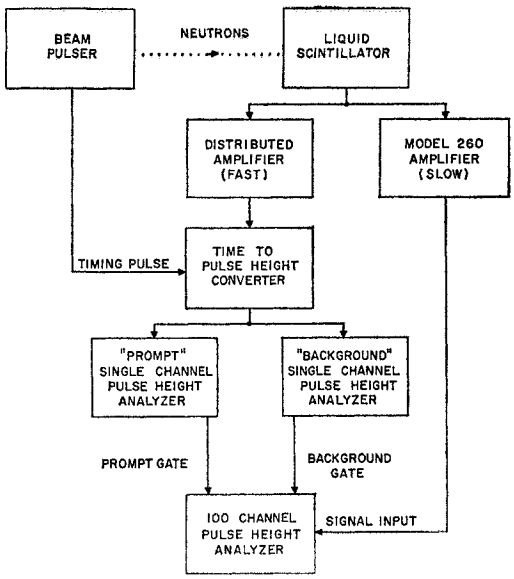

FIG. 4. Schematic arrangement of electronic equipment for measuring pulse-height distributions of capture pulses.

The arrangement of electronic circuits used in this part of the experiment is shown in Fig. 4. The time-to-pulse-height conversion is done exactly as previously described; the chief difference from Fig. 2 is that the converter output is now used as gate pulses to trigger the pulse-height analysis of the liquid scintillator output. Only those scintillator pulses are analyzed which occur at the proper times, corresponding to prompt events for captures, or to earlier events for background determination.

An additional necessary complication is that the background pulse-height distribution must be taken, for each sample, essentially simultaneously with the data on prompt pulses. It is desirable that these two distributions be taken over the same time interval because of the variation of background with neutron flux and with time, and because of possible gain changes in the circuits. This precaution is especially important for the lower energy pulses, corresponding to 1 to 3 Mev of gamma radiation, since the background of 2.2-Mev pulses may be comparable to the number of sample capture pulses in this region. For this reason, the 100-channel pulse-height analyzer was modified so as to act somewhat like two 50-channel analyzers. The

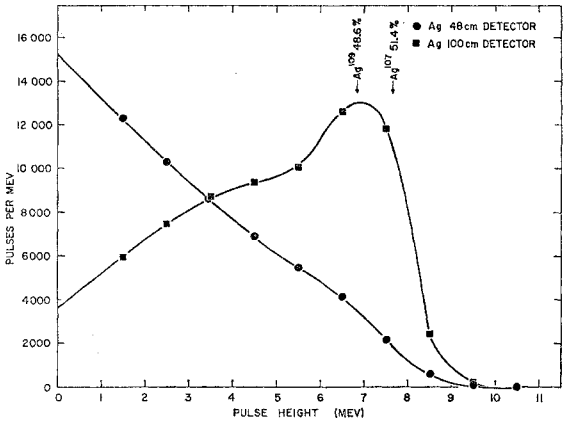

FIG. 5. Capture pulse-height distributions obtained for Ag in 48-cm and one-meter detectors. Background has been subtracted. The arrows indicate expected total gamma-ray energy for 400-kev neutrons.

same analyzing circuit analyzed pulses occurring both at prompt time and earlier, but separate gate inputs and information storage areas were necessary.

It was necessary to make sure that prompt and background pulse-height distributions corresponded to time intervals of equal length and were recorded with equal efficiency, so that the background distribution could be correctly subtracted. The basic method for ensuring this was to take data periodically with a radioactive source of random pulses replacing the time-correlated neutron source. Finally, prompt pulse-height distributions were taken for the polyethylene scatterer in order to subtract the effects of scattered neutrons from the capture sample distribution.

By this method pulse-height distributions were obtained for every element studied, for the pulse-height interval from 1 to 12 Mev. The energy calibration of pulse heights was performed daily by the use of a Pu-Be neutron and 4.4-Mev gamma source, and of a Co^{60} 1.17- and 1.33-Mev gamma-ray source. The pulse-height distributions for capture in Ag and Cd are shown in Figs. 5 and 6, as measured in both 48-cm and 100-cm scintillators. The 48-cm diameter scintillator has been described in an earlier paper.[35] It is obvious that the larger scintillator absorbs more of the gamma-ray energy and produces a better pulse-height distribution. However, in either case, the distributions obtained, extrapolated to zero pulse height, allow calculation with reasonable accuracy of the fraction of all capture pulses which would be accepted by the discriminator (single-channel pulse-height analyzer of Fig. 2) when set for the 3- to 12-Mev interval.

Also indicated in Figs. 5 and 6 are the expected total gamma-ray energies, which are equal to the tabulated neutron binding energies[42] plus the 400-kev kinetic energy of the incident neutron. In cases, such as Cd, in which considerably different binding energies are found among the naturally abundant isotopes, two or more peaks are obviously present in the pulse-height distribution.

The background pulse-height distribution which has been subtracted from these distributions is similar to that shown in Fig. 7, except that more 2.2 Mev and larger pulses are present when neutrons are being scattered by a sample. The number of such pulses varies from sample to sample and is kept at the level which permits the best accuracy in the capture pulse-height distribution. The main background in the 3- to 12-Mev region is presumably due to neutron capture in the iron of the scintillator tank, although there may also be some effect due to capture in the lead shielding. Neutrons produced by cosmic rays are largely responsible for the capture pulses shown in Fig. 7. Cosmic rays also produce numerous pulses of several hundred Mev in the scintillator tank. The natural radioactivity of K^{40} is presumably responsible for the pulses of about 1.46 Mev; the glass in the photomultipliers should contribute several hundred counts per second from this source.[43]

From all sources of constant background the 1-meter scintillator has about 1100 counts per second above 1 Mev in height, 500 per second above 3 Mev, and 350 per second above 10 Mev. Background at this rate is not very troublesome; for instance, a 1-μsec gate will have only 0.015% chance of containing a background pulse between 3 and 12 Mev. However, the effect of scattered neutrons will normally increase these rates by a factor of 2 or more.

Figure 8 shows all of the capture pulse-height distributions for the 1-meter scintillator which have been obtained with reasonable statistical accuracy, which usually requires a capture cross section greater than 20 mb in this experiment. In general, the distributions

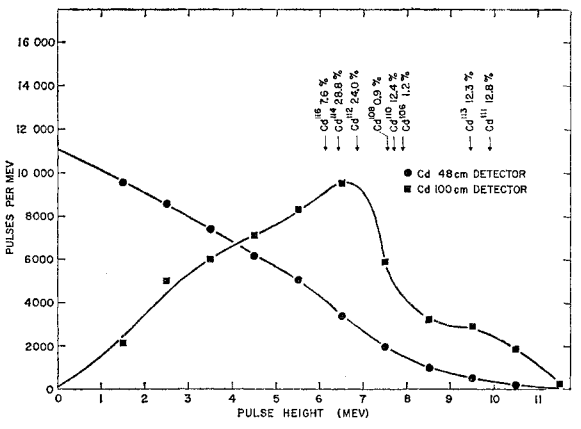

FIG. 6. Capture pulse-height distributions obtained for Cd in 48 cm and one-meter detectors. Background has been subtracted. The arrows indicate expected total gamma-ray energy for 400-kev neutrons.

[42] A. H. Wapstra, *Handbuch der Physik* (Springer-Verlag, Berlin, 1958), Vol. 38/1, pp. 1–37.

[43] E. C. Anderson (private communication).

are similar, with the exception of the exact positions of the peaks (which depend on the binding energy) and the fraction of counts below 1 or 2 Mev. This last factor should depend strongly on the effective multiplicity of the gamma rays emitted upon neutron capture. If, in an appreciable fraction of captures, nearly all the energy is emitted in a single high-energy gamma ray, it would be expected that in these cases only a fraction of the gamma-ray energy would be deposited in the scintillator, giving a broad pulse-height distribution. On the other hand, captures accompanied by many gamma rays of small energy in cascade should produce sharper pulse-height distributions with very few low-energy pulses, as may be readily calculated from the known cross sections for gamma-ray interactions. Examples of such high multiplicity are evidently Mo, Cd, and U^{235}, as seen in Fig. 8. However, the U^{235} events are mostly fission, not capture. It is known that fission usually results in many low-energy gamma rays[44–46] (total energy averaging about 8 ± 1 Mev, multiplicity about 8). The fact that the total energy of fission gamma rays varies from event to event accounts for the unusually large range of pulse heights for this case.

In the cases of Mo and Cd capture there is not sufficient information from other sources to verify the prediction of high effective multiplicity, based on the low percentage of small pulses. Although the spectrum produced by thermal capture in Cd^{113} is well known,[32,33] this isotope should account for only a minor portion of the captures which occur in Cd for fast neutrons. A similar situation holds for Mo neutron capture. However, thermal neutron capture in Au (100% Au^{197}) is known to produce many high-energy transitions (30% within 1 Mev of the ground-state transition energy) and to have a high average energy for capture gamma rays. This agrees with the pulse-height distribution observed for fast capture in Au. A similar though less well-defined situation exists for all of the heavy nuclides ($A>180$) represented in Fig. 8. This is in contrast to the generally lower-energy capture gamma rays from the medium-weight elements investigated. In the case of Nb (100% Nb^{93}) about 2% of thermal captures produce gamma rays within 1 Mev of the binding energy, and in the case of In (95.8% In^{115}) about 1.4%, with obvious results on the pulse-height distribution. The 100% abundant isotope Rh^{103}, on the other hand, produces gamma rays within 1 Mev of the binding energy in about 5% of all thermal neutron captures, with the pulse-height distribution agreeing. It would be expected from Fig. 8 that I^{127} capture produces more than the usual number of high-energy transitions, and this remark has recently been verified.[47]

Thus, to the extent that capture gamma-ray spectra

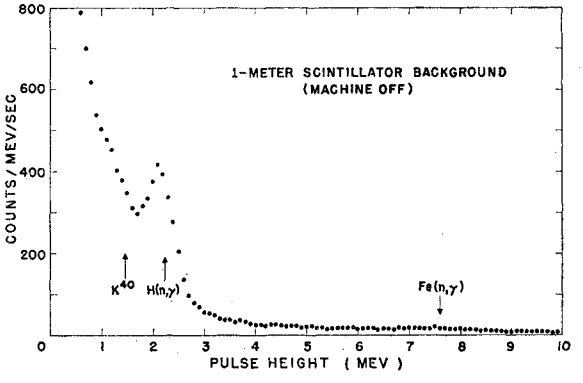

FIG. 7. Typical scintillator background pulse-height distribution for no pulsed neutron flux. The arrows indicate total gamma-ray energy for thermal capture of background neutrons in Fe^{56} and H^1, and for K^{40} radioactivity in the photomultiplier tubes.

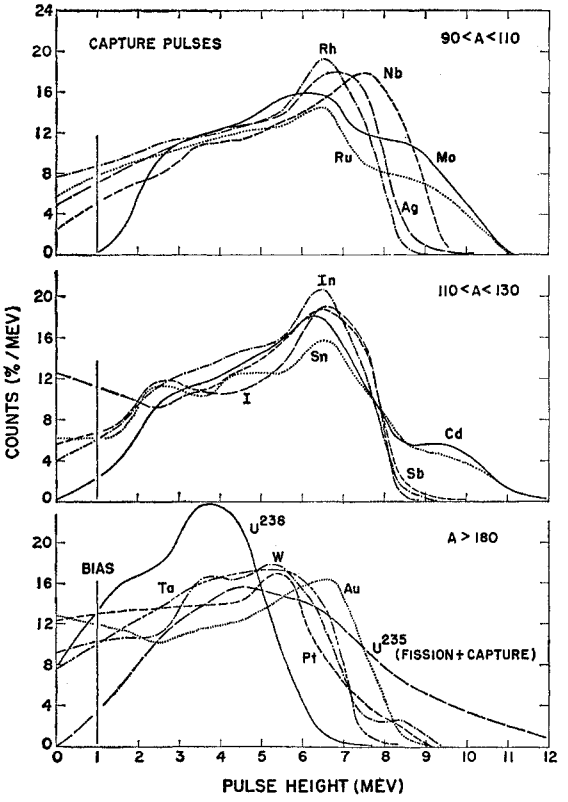

FIG. 8. Pulse-height distributions for capture events in 16 elements in the one-meter scintillator. For U^{235}, both fission and capture events are included. Background has been subtracted. Below 1 Mev the distributions represent extrapolations, not data.

[44] F. C. Maienschein, R. W. Peelle, W. Zobel, and T. A. Love, *Proceedings of the Second United Nations International Conference on the Peaceful Uses of Atomic Energy, Geneva, 1958* (United Nations, Geneva, 1958), Vol. 15, p. 366.

[45] A. B. Smith, P. R. Fields, and A. M. Friedman, Phys. Rev. **104**, 699 (1956).

[46] H. R. Bowman and S. G. Thompson, *Proceedings of the Second United Nations International Conference on the Peaceful Uses of Atomic Energy, Geneva, 1958* (United Nations, Geneva, 1958), Vol. 15, p. 212.

[47] H. Knoepfel, P. Scherrer, and P. Stoll, Z. Physik **156**, 293 (1959), report that 6.4% of thermal neutron captures in I^{127} produce quanta with energy within 1 Mev of the binding energy, and 12.6% are within 1.21 Mev.

are known in detail, the statements made above about the relation between pulse-height distribution and the gamma spectra are verified. This is also true of the total binding energies, which correspond (after adding 400 kev neutron kinetic energy) with the positions of the peaks in Figs. 5, 6, and 8. The only apparent exception is U^{238}, for which the peak is about 1 Mev too low, but this spectrum is obtained with reduced statistical accuracy because of radioactivity. Thus the pulse-height distributions can give information, or verification, on neutron binding energies, and even on the relative capture cross sections of isotopes with different binding energies. In the cases of Mo, Ru, Cd, Sn, and W, it may be determined readily that isotopes with both high and low binding energies have similar capture cross sections.

The pulse-height distributions discussed above allow the determination of that fraction of all capture pulses which is accepted by the discriminator when set for the 3- to 12-Mev interval. With this information it is possible to determine the number of capture events in the sample which caused a pulse in the detector.

C. Total Escape of Capture Gamma Radiation

It is possible that some capture events would be missed entirely because none of the capture gamma rays interact with the scintillator. This is only likely for those captures in which all of the available energy is released in a single gamma ray. In order to obtain a measure of the efficiency of the scintillator, all measurements were made on each element with two scintillators. One scintillator is 49 cm in diameter and 48 cm long, with a 6.4-cm-diameter axial hole; the other is 1 meter in diameter and length with a 7.0-cm aperture. The probability that a single 6-Mev gamma ray will escape from the 1-meter detector without undergoing Compton scattering or other interaction is about 34%, approximately the square of the 58% probability of this occurrence in the 48-cm detector. For 1-Mev gamma rays the corresponding figures are 6% and 24%, with still lower escape probabilities for lower energies. For more than one gamma ray emitted per capture these losses are greatly reduced, however. For the 1-meter scintillator the probability for total escape of two 3-Mev gamma rays is 4%, and for three 2-Mev gamma rays it is 0.3%. The loss would be even less for unequal division of the energy between the several gamma rays, as can be easily determined. Also, a gamma ray which has undergone a single Compton scattering has a high probability of depositing additional energy in the scintillator because of its reduced energy. Thus a capture gamma-ray multiplicity of 3 or more leads to an efficiency greater than 99% for the production of a scintillator pulse in the 1-meter detector. It is also evident that the probability of a small pulse—say less than 1 Mev—is more or less proportional to the probability that a single quantum may carry nearly all of the energy released by capture, since events of high gamma-ray multiplicity produce few such pulses.

Since the pulse-height measurements described are not easily extended below 1 Mev, it is necessary to assume that an extrapolation of the measured distribution below this value will give reasonably correct results for the fraction of capture pulses missed at 1-Mev bias. Simple numerical calculations of the pulse spectrum indicate that this assumption is reasonably correct.

Knowledge of the relative efficiencies of the two scintillators for detecting capture gives some information as to the fraction of capture events missed entirely by the scintillators. If all capture events from a given sample resulted in gamma rays of a single energy and multiplicity—say three 2-Mev gamma rays—it is readily verified that the losses in a large spherical tank having just twice the dimensions of a smaller tank would be given by the square of the losses in the smaller tank. Furthermore, if the ratio of efficiencies is $1+\delta$ in such a case, the efficiency of the larger tank is precisely given by $1-\delta^2$. The situation is slightly different for a spread in gamma-ray energies, such as 4-Mev and 2-Mev gamma rays in cascade, and quite different for variation in the multiplicity of gamma rays. Thus, if 10% of the captures resulted in a single gamma ray and the rest of the captures produced many gamma rays in cascade, virtually all of the losses would be due to the 10% of low-multiplicity captures. In such a case the ratio of efficiencies of the two scintillators would give little information on the absolute efficiencies. However, if it is specified that the losses are entirely due to 6- or 7-Mev quanta, the ratio of efficiencies $1+\delta$ can be shown to correspond, with reasonable accuracy, to an efficiency $1-\delta$ for the larger scintillator. This relation does not hold true in general, but is approximately correct for the scintillator sizes used.

The experimental ratios of numbers of detected capture events in the two scintillators are given in Table I for all elements observed to have 400-kev cross sections of more than 20 mb (except U^{238}, because of radioactive background); smaller cross sections lead to similar ratios, less accurately determined. These ratios include correction for counts below discriminator biases, and the errors are largely determined by uncertainty in this extrapolation below 1 Mev. The elements are arranged in order of increasing mass. The ratios are in agreement with conclusions drawn from pulse-height data and other information on capture-gamma-ray multiplicity. It is no surprise that the events with highest average multiplicity, capture and fission in U^{235}, are detected with the same efficiency, presumably essentially 100%, in both scintillators. It is also reasonable that Mo, Cd, Nb, In, and Ru, with ratios next nearest to 1.0, all have small numbers of low-energy pulses (see Fig. 8), and that I, W, Pt, Sn, and Au, with the largest ratios in Table I, should produce many low-energy pulses (with the exception of Sn).

The weighted average of all the ratios of efficiencies in Table I is $1.10=1+\delta$, excluding the obviously exceptional cases (see Fig. 8) of U^{235}, Mo, and Cd. The arguments given above then indicate that the average efficiency of the 1-meter scintillator for detecting capture should lie somewhere between approximately $1-\delta$ and $1-\delta^2$, or between 90% and 99%, depending on the multiplicity of the capture gamma-ray spectra involved. Because of the complicated and to some extent unknown nature of these matters, an arbitrary average efficiency of $95\pm5\%$ has been adopted for the correction of all 1-meter scintillator data, except that for U^{235}, Mo, and Cd. For these last three cases the efficiency has been taken as 100%.

D. Scattering Correction

Knowledge of the efficiencies for detecting captures, of the sample thicknesses, and of the relative numbers of captures detected in various samples, is not quite enough to permit the calculation of capture cross sections relative to a standard. An additional correction is necessary for the effects of scattering and attenuation of the neutron beam within the sample. True absorption of the neutron beam, by capture or fission, is very small for all samples used, and no correction has been made for it. In no case does it reduce the average flux by as much as 1%, and the effect is usually much less.

The effect which must be corrected for is the change in average path length due to scattering of neutrons. The neutron beam is attenuated by scattering in passage through the samples, but in many scattering events the thickness of sample traversed by a neutron is increased by the scattering. The analysis made is based on the assumption that scattering is isotropic, but it is estimated that the actual anisotropy of scattering will not appreciably change the result. In particular, the predominantly forward nature of scattering should not affect the average path length of scattered neutrons.

For a neutron scattered from the center of one face of a cylindrical disk of radius r and thickness t, assuming isotropy and no further interactions, the average path through the disk after scattering may easily be calculated to be

$$\bar{l}=(t/4)\ln(1+r^2/t^2)+(r/2)\tan^{-1}(t/r), \quad (1)$$

or

$$\bar{l}\cong(t/2)[1+\ln(r/t)]. \quad (2)$$

The approximate expression is valid for $t\ll r$, which is true for this experiment. By a simple extension of this calculation for neutrons scattered from points uniformly distributed along the axis of the disk, the average path length after scattering is given by

$$\bar{l}\cong(t/2)[(3/2)+\ln(r/t)], \quad (3)$$

also valid for $t\ll r$.

The assumption of no secondary interactions cannot be accurate in the present experiment, since the radii of the disks are about the same as the mean free paths for interaction of the neutrons in the sample materials. For this reason a cutoff has been put on the radius used in Eq. (3), on the assumption that a neutron scattered nearly parallel to the disk surfaces, which undergoes a second scattering within the disk, will usually leave the disk without further appreciable travel. This cutoff procedure involves the substitution, for r in Eq. (3), of $\lambda[1-\exp(-r/\lambda)]$, the mean free path length for maximum path length r; λ is the mean free path for infinite medium ($r=\infty$). This cutoff reduces the value of $\bar{l}$ from Eq. (3) by perhaps 10%, so that it is not a large effect under the conditions of this experiment, since ordinarily most neutrons are not scattered at all.

In many cases most of the path length of scattered neutrons is in disks other than the one in which scattering occurred. This is always the case for many closely spaced disks. For an isotropic neutron source on the axis of a sample disk, but at a distance s from the disk, the average path length is readily found by differentiating Eq. (1) to be

$$\bar{l}\cong(t/4)\ln[1+(r^2/s^2)]. \quad (4)$$

This equation is valid for $t\ll s$, which is always the case in the present experiment. Using these equations, the average path length for scattered neutrons has been calculated for scatterings in each of the disks of every sample, and averaged throughout each sample.

All of the equations above assume that the scattering occurs on the axis. In actuality the neutron flux is approximately uniform over a 1.9-cm diameter in the centers of the 3.80-cm diameter disks, but this would make no appreciable difference in the average path of scattered neutrons. Similar considerations have been given by Schmitt[48] for the somewhat different geometry used in capture experiments at Oak Ridge National Laboratory,[40] in which a single large disk of diameter up to 15 cm was used.

The mean free paths λ used in the present calculations

TABLE I. Ratio of the number of 400-kev captures producing pulses in the 1-meter scintillator, extrapolated to zero pulse height, to the number produced in the 48-cm scintillator, for identical irradiations. In the case of U^{235} most of the pulses are produced by fission rather than by capture. These ratios are related to gamma-ray multiplicity (see text).

Element	Ratio	Element	Ratio
Rb	1.07±0.14	Sn	1.15±0.15
Nb	1.04±0.13	Sb	1.08±0.13
Mo	0.99±0.10	I	1.18±0.15
Ru	1.06±0.10	Ta	1.12±0.14
Rh	1.09±0.13	W	1.17±0.14
Ag	1.11±0.13	Pt	1.15±0.19
Cd	1.03±0.10	Au	1.14±0.18
In	1.05±0.12	U^{235}	1.00±0.05

[48] H. W. Schmitt, Oak Ridge National Laboratory Report ORNL-2883, January, 1960 (unpublished).

TABLE II. Neutron capture cross sections in millibarns, normalized to the capture-plus-fission cross section of U^{235}. Neutron energy spreads are indicated; uncertainties in cross sections are discussed in the text. The capture cross section of U^{235} is from reference 35.

Neutron energy (kev)	175±25	250±40	400±90	600±75	800±66	900±63	1000±60
Ca	...	...	0.9± 0.5	...	...	...	...
Ti	5.3	5.3	4.0± 1.0	3.9	3.7	3.4	2.7
Cr	5.5	4.4	4.0± 1.5	4.0	4.8	3.6	3.7
Fe	5.8	6.9	4.9± 1.0	5.6	5.3	3.5	3.1
Ni	7.2	9.4	8.0± 1.5	8.0	7.4	6.8	7.2
Cu	17.8	18.7	15.4± 3	15.4	14.0	12.7	12.7
Zn	21.8	20.5	20.0± 2	19.7	20.5	19.0	17.0
Rb	...	...	52 ± 7	...	...	...	...
Y	...	...	7 ± 3	...	...	...	...
Zr	10.1	16.6	12.4± 2	12.8	12.7	11.6	7.1
Nb	79	78	65 ± 6	59	55	43	35
Mo	60	60	48 ± 5	48	39	30	30
Ru	177	155	109 ±11	72	56	50	50
Rh	416	339	186 ±19	129	94	84	81
Ag	466	392	227 ±23	180	146	133	125
Cd	...	...	101 ±11	...	...	...	...
In	362	318	297 ±33	297	320	303	314
Sn	50	50	41 ± 4	45	51	47	55
Sb	152	137	126 ±12	115	119	116	122
I	...	...	176 ±15	...	...	...	...
Ce	...	...	8 ± 3	...	...	...	...
Ta	375	304	247 ±23	194	170	153	160
W	130	130	100 ±16	98	100	100	114
Pt	251	202	129 ±15	101	91	91	84
Au	326	272	206 ±18	138	111	97	104
Pb	6.2	3.6	4.0± 1.5	4.6	3.6	3.3	3.3
Bi	...	...	2 ± 3	...	...	...	...
U^{238}	174	172	151 ±25	174	203	208	223
$U^{235}(\sigma_c)$	268±33	227±30	184 ±17	160±19	107±15	107±12	92±16
$U^{235}(\sigma_f+\sigma_c)$	1820	1670	1500	1370	1290	1300	1400

are calculated from the actual amount of scattering produced by each sample, as determined from the background counts; these values agree well with published cross-section data.[24] Samples scattering about 10% of the neutrons passing through them were used for all elements having capture cross sections larger than about 80 mb, with the exception of I (for which a NaI sample giving about 26% scattering was used). For scattering of about 10% the path-length correction factor used (ratio to path for no scattering) varied from 0.98±0.02 for 20 disks to 1.02±0.02 for three disks.

For elements with capture cross sections in the range 14 to 80 mb, samples scattering about 20% of the neutron flux were used, with the exception of Rb (for which a RbF sample scattering about 66% was used). For these samples, path length correction factors ranged from 0.96±0.03 for 10 disks to 1.00±0.03 for four disks.

For those elements with cross sections less than 14 mb, samples scattering up to 66% were used, with correction factors as low as 0.76±0.05. It is estimated that for every element investigated in this experiment the uncertainties in scattering corrections are small compared to other sources of error.

III. RESULTS

The measurements and corrections described above are sufficient to determine the absolute numbers of captures which occur in the various samples used. By rapid and repeated interchange of samples it is possible to ensure that all samples are exposed to the same neutron flux. Thus relative capture cross sections may be determined, and all cross sections may be put on an absolute basis if one absolute cross section is well known. The standard which has been chosen is the cross section for capture plus fission in U^{235}, since this is more accurately known than any of the capture cross sections, and since captures and fissions are both detected with the same efficiency, nearly 100%.

The resulting absolute cross sections are given in Table II. Also tabulated are the cross sections of the standard, U^{235}, as derived from fission cross-section data summarized by Allen and Henkel,[49] as well as by

[49] W. D. Allen and R. L. Henkel, *Progress in Nuclear Energy* (Pergamon Press, New York, 1958), Ser. I, Vol. 2, p. 1.

Hughes and Schwartz,[24] and from the data on $\alpha=\sigma_c/\sigma_f$ reported by Diven, Terrell, and Hemmendinger.[35]

The estimated standard deviations given in Table II include uncertainties in extrapolation of the pulse-height distributions to zero pulse height, in the scintillator efficiency at zero pulse height as estimated from ratios of counts in two scintillator tanks, in the scattering correction, and statistical uncertainties. Only in the cases of very small cross sections, where background levels limited counting accuracy, were statistics important.

Measurements were made at seven neutron energies from 175 to 1000 kev, with energy spreads approximately equal to the energy steps. The uncertainties in cross sections are given only at 400 kev because the pulse-height data, associated with the most uncertain correction, were taken only at that energy. At other energies the capture pulse-height distribution and the scattering correction are presumably little changed, and the uncertainties in measured cross sections relative to the 400-kev value are due mostly to statistical errors and various instrumental factors. It is estimated, partly on the basis of reproducibility of data, that the relative errors in these cross sections, disregarding normalization at 400 kev, are approximately 7% or 1 mb, whichever is greater.

Figures 9 and 10 show these results as functions of energy in the cases where measurements were made at more than one energy, with relative standard deviations as discussed above. Figure 11 shows the 400-kev cross sections as functions of the average mass A of the target elements. The curve is included merely to guide the eye and is without theoretical significance.

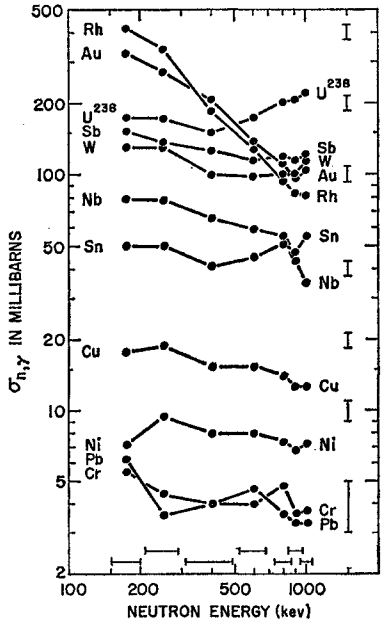

FIG. 9. Neutron capture cross sections for 11 elements as functions of neutron energy. Relative standard deviations of the cross sections and neutron energy spreads are indicated. For absolute standard deviations, see Table II.

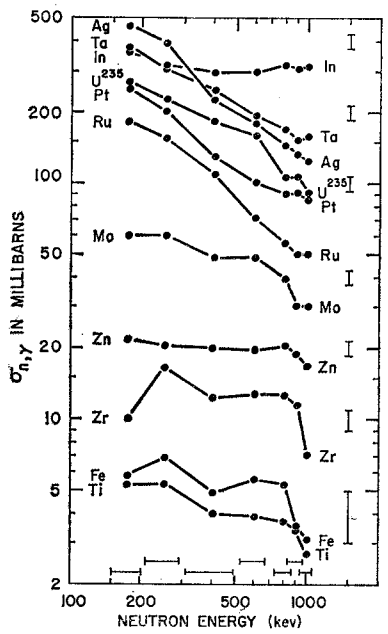

FIG. 10. Neutron capture cross sections for 11 elements as functions of neutron energy. Relative standard deviations of the cross sections and neutron energy spreads are indicated. For absolute standard deviations, see Table II.

IV. DISCUSSION

In this section it will be shown that the measured capture cross sections are in general agreement with the predictions of resonance theory, without attempting to consider details of the level structure of each nucleus. The level densities will be assumed to be those of the Fermi gas model, with excitation measured from the effective ground state of Hurwitz and Bethe. No attempt will be made to achieve precision greater than a factor of two in these general considerations. It is hoped that these ideas will be useful where information needed for a precise calculation is incomplete, as is usually the case.

The neutron capture cross section in the vicinity of a single isolated resonance is given by resonance theory[50-55] as

$$\sigma(n,\gamma)=\sum_l \frac{(2l+1)\pi\lambda^2 g\Gamma_{nl}\Gamma_\gamma}{(E-E_r)^2+\Gamma^2/4}. \quad (5)$$

[50] H. Feshbach, D. C. Peaslee, and V. F. Weisskopf, Phys. Rev. **71**, 145 (1947).

[51] J. M. Blatt and V. F. Weisskopf, *Theoretical Nuclear Physics* (John Wiley & Sons, Inc., New York, 1952), pp. 379 ff.

[52] A. G. W. Cameron, U. S. Atomic Energy Commission Report TID-7547 (Office of Technical Services, Department of Commerce, Washington, 1957), pp. 68–71.

[53] L. Dresner, U. S. Atomic Energy Commission Report TID-7547 (Office of Technical Services, Department of Commerce, Washington, 1957), pp. 71–76.

[54] A. M. Lane and J. E. Lynn, Proc. Phys. Soc. (London) **A70**, 557 (1957).

[55] E. R. Rae, B. Margolis, and E. S. Troubetzkoy, Phys. Rev. **112**, 492 (1958).

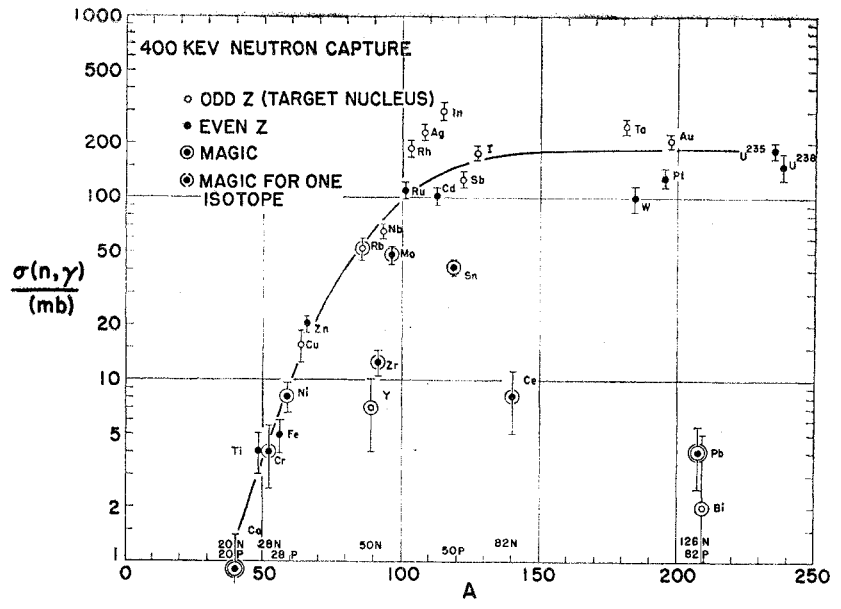

FIG. 11. Neutron capture cross sections at 400 kev, plotted against average mass of target nucleus. The curve is intended only to guide the eye.

In this equation E, λ, and l are the kinetic energy, reduced wavelength, and angular momentum of the incident neutron, E_r is the resonance energy, and Γ, Γ_γ, and Γ_{nl} are the total, radiation, and partial neutron widths of the level. The statistical weighting factor g is defined here by

$$g=(2J+1)\epsilon/2(2I+1)(2l+1), \tag{6}$$

and is the probability that the neutron spin $s=\frac{1}{2}$ and angular momentum l will combine with the target nucleus spin I to form a compound nucleus spin J. It should be noted that in this paper the factor $(2l+1)$ is included in g, so that $\sum_J g=1$ and g is the absolute, not relative, probability. The factor ϵ is the number of channel spins (resultants of I and s) which can yield the value of J in question; it was introduced by Hauser and Feshbach.[56] If the value of J cannot be obtained by combining I, l, and s, then $\epsilon=0$. For $l=0$ or $I=0$ the weighting factor ϵ can only be 0 or 1; in general it can be 0, 1, or 2.

For well-separated levels (without appreciable overlap) the average of Eq. (5) over many resonances is

$$\langle\sigma(n,\gamma)\rangle=\sum_l 2(2l+1)\pi^2\lambda^2\langle g\Gamma_{nl}\Gamma_\gamma/\Gamma\rangle_l\omega_l, \tag{7}$$

in which ω_l is the density of levels (per unit energy) which can be excited by a given l value, and the quantity within brackets is averaged over these levels.

The product $\langle g\rangle_l\omega_l$ is to a large extent independent of l. For $l=0$, levels of two different values of J may be excited, for $I>0$, and the value of $\langle g\rangle_s\cong\frac{1}{2}$; for $l=1$, four different J values are involved, for $I>1$, and $\langle g\rangle_p\cong\frac{1}{4}$. In general, unless $l\gg I$, the number of possible J values for given l is approximately the inverse of $\langle g\rangle_l$, so that $\langle g\rangle_l\omega_l$ is nearly independent of l. All these approximate relations would be exact if the level density were independent of J. This statement follows from the simple observation that if, for given l, n different values of J may be produced, each corresponding to an equal number of levels, the weighted average $\langle g\rangle_l=1/n$. However, it is usually assumed that the level density is proportional to $(2J+1)$, and this gives the higher J values, and hence larger g values, more weight in the average. For large values of I the $(2J+1)$ weighting would make almost no difference in $\langle g\rangle_l$, and even for small values of I the weighting would not have a large effect.[57] Because of this, and for simplicity, the possible $(2J+1)$ factor in the level density will not be considered here, although it would have an obvious effect on the cross section.

The s-wave contribution to the capture cross section should vary as $E^{-\frac{1}{2}}$ at very low energies, since Γ_{n0} is predicted by theory[51] to vary as $E^{\frac{1}{2}}$. At higher energies, when $\Gamma_{n0}\gg\Gamma_\gamma$, the s-wave contribution should vary as E^{-1}. It is apparent from Figs. 9 and 10 that neither of these slopes is in general correct for the few-hundred-kev region, and in some cases (e.g., U^{238}) the slope is even of opposite sign. There are a number of elements having high capture cross sections for which the cross section approaches E^{-1} dependence, but usually the slope is less, particularly for low cross sections. Similar results have been obtained by other groups.[24,27,40] Where both s- and p-wave contributions are important, the simple E^{-1} variation does not apply, and the increase of level density with energy may also alter the slope. It would be expected that higher l values would be of

[56] W. Hauser and H. Feshbach, Phys. Rev. 87, 366 (1952).

[57] For $I=0$, for example, the quantities $\langle g\rangle_l\omega_l$, assuming a $(2J+1)$ level density factor, are in the ratio 1:5/3:13/5 for $l=0$, 1, 2. For $I=\frac{1}{2}$ the ratios are: 1:22/15:54/25, and for $I=1$ they are 1:19/15:43/25. For large values of I, $\langle g\rangle_l\omega_l$ is almost independent of l.

greater importance, resulting in less slope, for those nuclides having neutron widths relatively large compared to radiation widths. Nuclear theory would predict,[50] on the basis of an inverse relation between level widths and densities, that this would be the case for those nuclides having unusually low level densities and hence low capture cross sections. This is in agreement with the general correlation of slopes and cross sections seen in Figs. 9 and 10, and has been pointed out also by Johnsrud et al.[27]

The number of terms in Eq. (7) which make large contributions to the capture cross section increases with neutron energy because of the more rapid increase with energy of Γ_{nl} than Γ_γ. So long as several different l values do not yield comparable neutron widths for the same level, and inelastic scattering may be neglected, which requires that the energy be limited, the partial neutron width then becomes nearly equal to the total level width. In this situation the factor $\Gamma_{nl}\Gamma_\gamma/\Gamma \rightarrow \Gamma_\gamma$ with increasing neutron energy. This "saturation" means that for these l values the neutron width or strength function is no longer of much significance. For the region of a few hundred kev, s- and p-wave neutrons should account for most of the capture cross section, and both contributions should be nearly saturated, so that the capture cross section may be written as

$$\langle\sigma(n,\gamma)\rangle \cong 2\pi^2\lambda^2\langle g\Gamma_\gamma\rangle_s\omega_s + 6\pi^2\lambda^2\langle g\Gamma_\gamma\rangle_p\omega_p. \quad (8)$$

Thus, neglecting inelastic scattering, the capture cross section in this region is more or less proportional to the product of the radiation width and level density. This last conclusion is, of course, not a new one.[18,58] A similar argument can be made for the region of a few kev, where the cross section is mostly due to s-wave neutrons.

The radiation width is known to be of the order of 0.1 ev for a wide range of nuclides, for low-energy neutron capture. It is expected to increase with excitation energy, but this should not be an important effect for a few hundred kev. Weisskopf has estimated on a semiclassical basis that the electric-dipole radiation width should be the dominant factor, and that it should be proportional to E^3R^2, in which E is the gamma-ray transition energy and R is the nuclear radius. It appears that most initial capture gamma transitions are of the E_1 type.[59,60] The transition energy, on the basis of the usual Fermi gas model of level densities, should be given by a small factor (about 2) times the nuclear temperature[61] $T=(E_e/a)^{\frac{1}{2}}$. Here E_e is the effective excitation energy as used by Hurwitz and Bethe,[62]

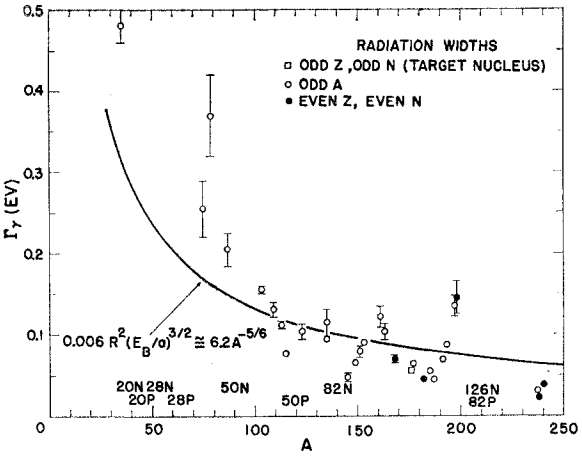

FIG. 12. Radiation widths known to 15% uncertainty or better, from the compilation of Stolovy and Harvey. The curve is theoretical, with coefficient arbitrarily chosen to fit the data.

measured from an effective ground state, lying above the actual ground state for even-even or magic-number compound nuclides. The nuclear temperature coefficient[63–65] is given by both theory and experiment as

$$a \cong A/10. \quad (9)$$

Hence, on the basis of these estimates,

$$\Gamma_\gamma \cong \text{const.}T^3R^2 \cong \text{const.}E_e^{3/2}r_0^2A^{2/3}a^{-3/2} \cong \text{const.}E_e^{3/2}r_0^2A^{-5/6}. \quad (10)$$

The factors r_0 and A are, as usual, the nuclear radius constant and the nuclear mass number.

According to this the radiation width should vary more or less as $A^{-5/6}$, neglecting the variation of E_e. Perhaps surprisingly, this rough estimate fits the general trend of Γ_γ, as seen in Fig. 12, rather well. The data shown are a portion of those summarized by Stolovy and Harvey,[66] chosen on the basis of 15% or less uncertainty in radiation width. There are apparently systematic deviations from the smooth curve of Fig. 12 (the coefficient 0.006 is arbitrarily chosen to fit the data) which are not connected with evenness or oddness and not necessarily with magic numbers. However, the crude theoretical curve fits the data as well as any other suggested.[66–70] On the basis of this theory it would be expected that Γ_γ would be little changed by a few hundred kev change in incident neutron energy.

The most widely variable factor in the capture cross section, the level density, should be proportional to $\exp[2(aE_e)^{\frac{1}{2}}]$, according to the degenerate Fermi gas

[58] H. A. Bethe, Phys. Rev. **57**, 1125 (1940).
[59] B. B. Kinsey and G. A. Bartholomew, Phys. Rev. **93**, 1260 (1954).
[60] L. V. Groshev, A. M. Demidov, V. N. Lutsenko, and V. I. Pelekhov, *Proceedings of the Second United Nations International Conference on the Peaceful Uses of Atomic Energy, Geneva, 1958* (United Nations, Geneva, 1958), Vol. 15, p. 138.
[61] A similar conclusion may be obtained from reference 60.
[62] H. Hurwitz, Jr., and H. A. Bethe, Phys. Rev. **81**, 898 (1951).
[63] J. M. B. Lang and K. J. Le Couteur, Proc. Phys. Soc. (London) **A67**, 586 (1954); K. J. Le Couteur and D. W. Lang, Nuclear Phys. **13**, 32 (1959).
[64] T. D. Newton, Can. J. Phys. **34**, 804 (1956).
[65] J. Terrell, Phys. Rev. **113**, 527 (1959).
[66] A. Stolovy and J. A. Harvey, Phys. Rev. **108**, 353 (1957).
[67] J. Heidmann and H. A. Bethe, Phys. Rev. **84**, 274 (1951).
[68] D. J. Hughes and J. A. Harvey, Nature **173**, 942 (1954).
[69] J. S. Levin and D. J. Hughes, Phys. Rev. **101**, 1328 (1956).
[70] A. G. W. Cameron, Can. J. Phys. **35**, 666 (1957).

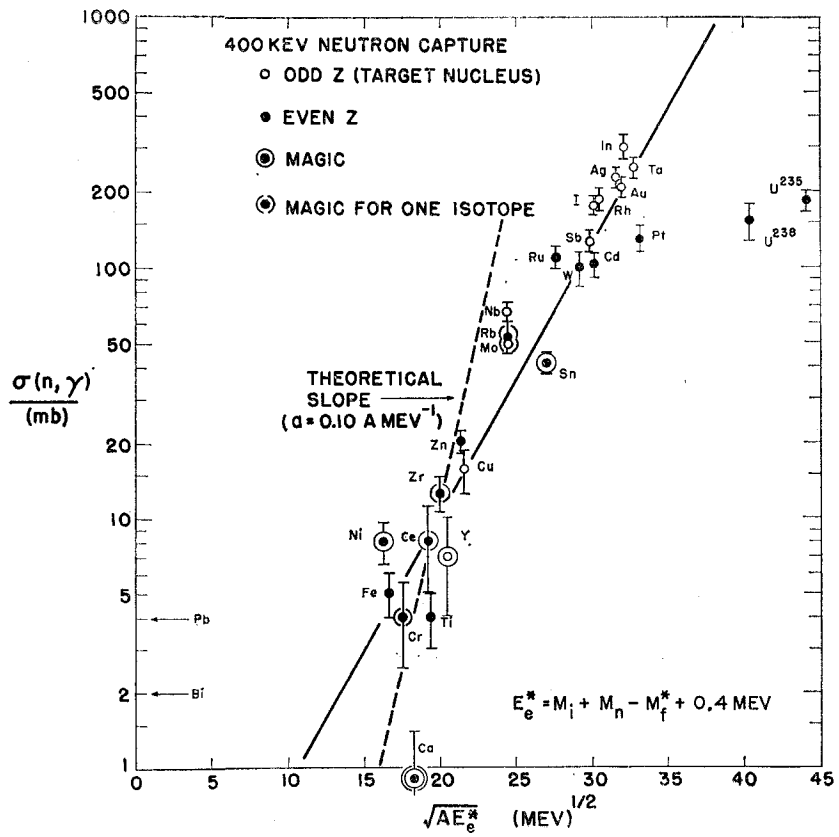

FIG. 13. Neutron capture cross sections at 400 kev, plotted against $(AE_e^*)^{\frac{1}{2}}$, the exponent in the usual level-density formula. The quantity E_e^* is the effective excitation energy, as discussed in the text. The heavy line is empirically drawn to fit the data.

model of the nucleus.[71] The excitation energy E_e should be measured from an effective ground state, according to the ideas of Hurwitz and Bethe.[62] This ground state should be given by a mass surface which is the same for even and odd numbers of protons and neutrons and which takes no account of magic number effects. The basic idea is that pairing and magic numbers have strong effects on the ground state and low-lying excited states, but little effect on higher levels; the density of the latter should not, then, depend very much on the actual position of the ground state, which is lowered by several Mev for magic-number or even-even nuclides.

Thus the capture cross section should depend strongly on the ground-state mass of the target nucleus, not of the compound nucleus. Magic-number and even-even target nuclides should yield unusually low effective excitations, level densities, and capture cross sections. That this is apparently correct has been pointed out elsewhere,[18,62] and is evident in Fig. 11, at least for magic-number target nuclides. The general trend of cross sections with A is given by the exponential level-density formula, with allowance for decreasing binding energy for heavier elements.

In order to put the ideas of Hurwitz and Bethe, and of the Fermi gas model of the nucleus, on a more quantitative basis, effective excitations produced by neutron capture have been calculated for every element investigated in this paper. The effective excitation was calculated for each isotope by use of the actual masses of the target nuclide and the incident neutron and a theoretical mass for the final nuclide. The mass surface used was based on Cameron's semiempirical formula,[72] without the shell or pairing corrections. Thus the calculated mass values for odd-odd, nonmagic-number nuclides were used for all final nuclides, in the hope that the level densities and capture cross sections depend mainly on excitation above these "effective" ground states. Where several target nuclides are present for a given element, the average effective excitation was used.

The results are shown in Fig. 13, in which the measured 400-kev neutron capture cross sections are shown as functions of $(AE_e^*)^{\frac{1}{2}}$. The effective excitation E_e^* for 400-kev neutron capture is calculated, as implied above, from the equation

$$E_e^*=E_b+M_f-M_f^*+E_n=M_i+M_n-M_f^*+E_n. \quad (11)$$

In this equation $E_b=M_i+M_n-M_f$ is the experimental binding energy for the captured neutron of incident energy E_n, and M_i, M_n, M_f, and M_f^* are, respectively,

[71] Reference 51, p. 371.

[72] A. G. W. Cameron, Chalk River Project Report CRP-690, Ontario, Canada, 1957 (unpublished); Can. J. Phys. 35, 1021 (1957).

the experimental masses of the initial nucleus, captured neutron, and final nucleus, and the calculated "reference" mass of the final nucleus as described above. It should be emphasized that the effective excitation calculated in this way requires no experimental knowledge of the mass of the final nucleus nor of the binding energy of the captured neutron. This procedure results in negative effective excitations for the magic elements Pb and Bi, so that they cannot be shown in the figure. It would be expected, however, that negative effective excitations would correspond to very low level densities and very small capture cross sections, and these expectations are correct for Pb and Bi.

The correlation of capture cross sections with $(AE_e^*)^{\frac{1}{2}}$, as seen in Fig. 13, is reasonably good. The use of an effective excitation energy accounts for most of the differences between magic-number and nonmagic-number nuclides and for the even-odd effects. For most nuclides the points fall within roughly a factor of 2 of the heavy straight line, which is quite arbitrarily drawn. The principal exceptions are the heaviest nuclides; it is possible that the mass surface used is not suitable in this region. The less variable factor Γ_γ has not been included here, for simplicity; if $\sigma(n,\gamma)/\Gamma_\gamma$ is plotted against $(AE_e^*)^{\frac{1}{2}}$ the points fall more nearly on a line having the slope approximately predicted by theory, given by $a \cong A/10$. The theoretical slope is even more closely attained by including the a^2E^2 factor which is usually[63,64,73] included in the denominator of the level density expression. However, these methods produce no better correlation than the simpler method of Fig. 13, and this figure may be of value in predicting an unknown capture cross section without precise knowledge of neutron strength functions and level densities.

The correlation shown in Fig. 13 should work fairly well, because for neutrons of a few hundred kev both s- and p-wave contributions should be nearly saturated, and thus more or less independent of neutron strength functions. It is not expected to be highly accurate because of the omission of variations of radiation width (see Fig. 12), d-wave and higher contributions, the possible $(2J+1)$ level density factor, and inelastic scattering.

V. CONCLUSIONS

The capture cross sections of a number of elements have been measured for neutrons in the energy range 175 to 1000 kev. The absolute cross sections have been determined by comparison with the known capture-plus-fission cross section of U^{235}, together with corrections for escape of capture gamma-radiation from the scintillator and for scattering of neutrons in the capture samples. The results appear to fit quantitatively, reasonably well, the predictions of resonance theory, together with the usual Fermi gas level densities and the Hurwitz-Bethe idea of depression of the ground state by magic-number and even-odd effects.

VI. ACKNOWLEDGMENTS

The authors wish to thank J. W. Jordan of this laboratory for much valuable help in construction of equipment and collection of data. We are also grateful for discussions with Dr. J. H. Gibbons, Dr. R. L. Macklin, Dr. P. D. Miller, Dr. J. H. Neiler, and Dr. H. W. Schmidt, of Oak Ridge National Laboratory, who are engaged in a similar experiment.

[73] H. A. Bethe, Phys. Rev. **50**, 332 (1936).